Radiation induced recharging of cerium ions in Nd, Ce: $Y_3Al_5O_{12}$ single crystals

S. M. Kaczmarek[1], D. J. Sugak[2], A. O. Matkovskii[2,3], Z. Moroz[4], M. Kwaśny[1], A. N.

Durygin[5]

1 - Institute of Optoelectronics, Military University of Technology, 2 Kaliski Str., 01-489 Warsaw, Poland
2 - Institute of Materials, SRC "Carat", 202, Stryjska St., Lviv 290031, Ukraine
3 - Institute of Physics HPS, 16A Rejtana St., Rzeszow 35 310, Poland
4 - So³tan Institute of Nuclear Studies, 05-400 Œwierk, Poland
5 - Institute of Physics, Polish Academy of Science, 32/46 Al. Lotnikow, 02 668 Warsaw, Poland

Corresponding author: S³awomir Maksymilian Kaczmarek, Institute of Optoelectronics, Military University of Technology, 2 Kaliski Str., 01-489 Warsaw, Poland, Phone: 6859019,   Fax: (4822) 6668950,
E-mail: laslab@wat.waw.pl

Abstract

Radiation induced reacharging of Ce^{3+} and Ce^{4+} ions in Ce and Nd doped yttrium-aluminium garnet crystals was observed. This effect depends on the Ce^{3+} ion concentration and the type of ionizing radiation. The crystals investigated were irradiated with gamma rays, protons with doses up to 10^{14} protons/cm^2 and electrons with a dose of $5*10^{16}$ electrons/cm^2. Changes in cerium concentration after gamma irradiation were calculated from the formula of Smakula.

PACS codes: 61.72.Ji, 61.80.Ed, 42.70.Iij

Keywords: additional absorption, gamma-irradiation, ionization, proton and electron beams, crystal growth, annealing

1. Introduction

It is known that colour centers in neodymium doped yttrium-aluminum garnet (YAG:Nd) crystals produced by the ultraviolet part of a pumping lamp spectrum as well as by bombardment by various types of ionizing particles (gamma-rays,

electrons, protons etc.) unfavourably influence the output characteristics of solid-state Nd: YAG lasers [1-3].
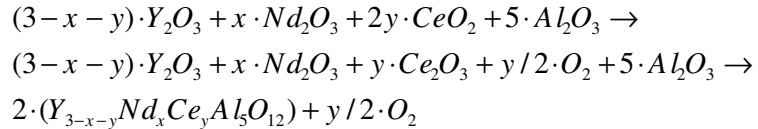
Many methods exist to make the optical characteristics of crystals less sensitive to irradiation. They are described e.g. in Ref [1]. In particular, in one such method, in addition to the ordinary Nd^{3+} dopant, the introduction of extra Ce^{3+} ions is performed during the process of crystal growth. This method appears to be extremely advantageous, because the Ce^{3+} ions, due to the energy transfer $Ce^{3+} \rightarrow Nd^{3+}$, may also improve the luminescence of the Nd^{3+} ions [4, 5].

It was shown in Ref [6] that the influence of Ce^{3+} ions on the radiation sensitivity of YAG:Nd crystals is somewhat ambiguous. Namely, with the increase of the concentration by weight of the Ce^{3+} ions from 0.05 to 0.1 % an additional absorption induced by radiation (labelled here as " AA") also increases. But, a further increase of this concentration (from 0.1 to 1 % by weight) causes an essential drop of the AA factor.

In the present work we attempted to study in more detail the influence of the gamma and proton radiation on the optical properties of the Ce, Nd: YAG crystals for various concentrations of Ce ions.

2. Experimental setup

The crystal samples were grown by the Czochralski method in iridium crucibles. The process was carried out in an N_2 atmosphere with the addition of a 2% admixture of O_2. As a starting material the oxides Y_2O_3, Al_2O_3, Nd_2O_3 and CeO_2 of at least 4N purity were used. First they were dried to remove water, weighed and then mixed mechanically. After that the mixture was heated in an aluminium container to produce the reaction:

$$(3-x-y)\cdot Y_2O_3 + x\cdot Nd_2O_3 + 2y\cdot CeO_2 + 5\cdot Al_2O_3 \rightarrow$$
$$(3-x-y)\cdot Y_2O_3 + x\cdot Nd_2O_3 + y\cdot Ce_2O_3 + y/2\cdot O_2 + 5\cdot Al_2O_3 \rightarrow$$
$$2\cdot(Y_{3-x-y}Nd_xCe_yAl_5O_{12}) + y/2\cdot O_2$$

It should be noted that during the heating a major part of the cerium ions should pass to the trivalence state. It is not excluded, however, that some of these ions remain in the Ce^{4+} state. For crystal growth a starting material was used, for which x=0.001, y=0.005.

To obtain samples with different concentrations of cerium, parallel crystal plates with a thickness of about 1 mm were cut-out from the suitable places of the conical part of the crystal, perpendicularly to the outgrowing < 111 > axis. These samples were labelled correspondingly as S1, S2, S3 and S4, beginning from the top of the crystal. One of the samples investigated, S5, was taken from another bulk crystal. Then, after cutting-out, the samples were polished to obtain optical quality, which was controlled by means of a Mach-Zehnder interferometer. Next, each sample was split into two parts: the first one was irradiaded by gamma-rays while the second one was heated for three hours in air at 1400 deg. Sample S4, after this annealing, was annealed in an N_2+H_2 mixture for 1,5 h and next γ-irradiated with a dose of 10^5 Gy. Sample S5, after this annealing, was irradiated by protons with doses of $1*10^{13}$, $3*10^{13}$ and $1*10^{14}$ protons/cm^2.

The spectral dependence of the absorption coefficient for the crystals was calculated from their transmission spectra, taking into account the effect of multiple reflection by the surfaces. The transmission spectra were recorded by means of the Perkin-Elmer spectrophotometer LAMBDA-2, in the range from 190 to 1100 nanometers. Values of AA factors due to the irradiation or thermal processing were calculated from the formula:

$$\Delta K = \frac{1}{d} \cdot \ln \frac{T_1}{T_2},$$

where d is the sample thickness and T_1 and T_2 are the transmissions of the sample obtained before and after gamma irradiation or thermal treatement, respectively.

The samples were irradiated by means of a ^{60}Co gamma source (average gamma energy 1.25 MeV) up to an absorbed dose of 10^5 Gy.

3. Results

In Fig 1 the absorption spectra for the samples S1,...,S5 are shown. It is seen that in wavelength range up to about 850nm, additional low-energy bands with maxima at 458 and 338 nm can be clearly distinguished. They correspond to the transitions between 4f-5d configurations in the Ce^{3+} ions. The remaining three bands, characteristic for the transitions 4f-5d in Ce^{3+} in the structure of the garnet [7], lay on the absorbtion edge of the crystal and are in the range 220-250 nm.

As can be guessed from Fig.1, when passing from the top of the crystal along the growth axis, the intensity of the absorption of Ce^{3+} bands increases, which indicates the growth of the cerium concentration.

It is known that there exists an unambiguous relation between the density of the absorption centers and the parameters of the absorption bands, which is expressed by the formula of Smakula, modified in ref. [8] for cases where the shape of the absorption line is described by Gaussian or Lorentzian distributions. Using this formula we calculated the total concentration of Ce^{3+} ions in the samples as well as relative change of Ce^{3+} concentration induced by the irradiation. For the calculations, the Ce^{3+} absorbtion band of 4f-5d transitions with the maximum at 458 nm was chosen, because according to [7] it has a Gaussian shape. In this case, the Ce^{3+} concentration can be calculated according to the formula:

$$N_{Ce} = 0{,}87 \cdot 10^{17}\,cm^{-3} \cdot K \cdot W \cdot [n / (n^2 + 2)^2] \cdot 1 / f_o ,$$

where K - is the the value of the absorption coefficient at the band maximum, expressed in cm^{-1}; W - is the FWHM of the absorption band, expressed in eV ; n - is the crystal refractive index for the wavelength corresponding to the maximum of the absorption band; f_0 - is the oscillator strength for a given transition.

Parameters K and W were obtained experimentally and they are presented in the table. The refractive index n = 1.847 was calculated from the relation:

$$n^2 - 1 = A \cdot \lambda^2 / (\lambda^2 - B),$$

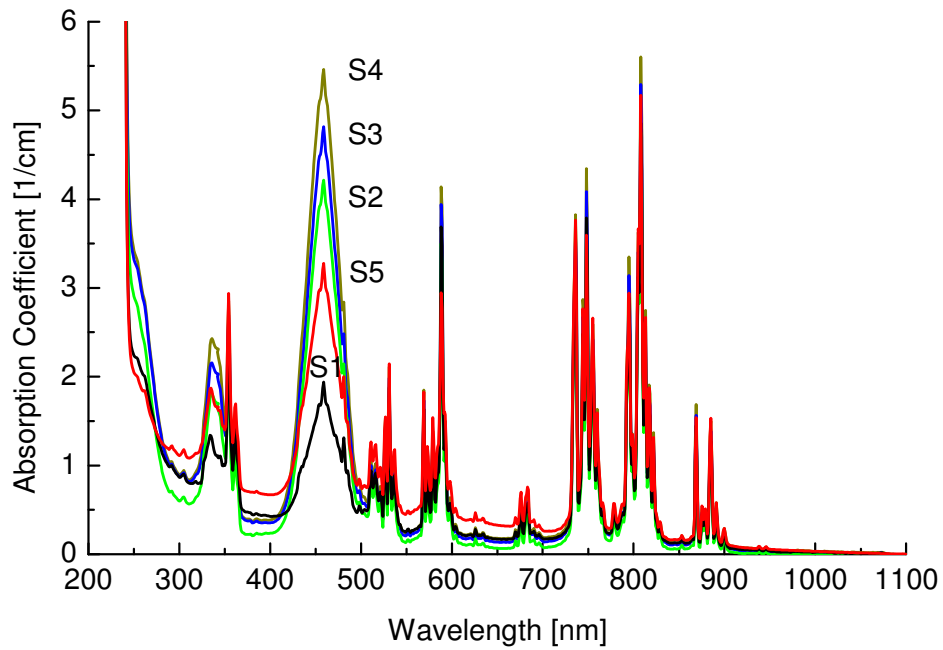where coefficients A=2.283 and B=0.01261 were obtained from experimental data published in [9].

Fig. 1.

To calculate values of N_{Ce} it was assumed that the corresponding oscillator strength is $f_0 = 3*10^{-3}$. This is based on the results of Ref [10], where the

oscillator strengths were calculated for the transitions between different configurations of Ce^{3+} ions in various types of oxides.

As seen from the table, when passing from the top along the axis of the crystal growth, the concentration of the Ce^{3+} ions increases. However, the calculations give somewhat lower values of cerium concentrations, as compared to those prepared in the starting material. This fact can be explained by incomplete penetration of the Ce ions into the crystal (due to a small value of their distribution coefficient : ~0.07), or by a not accurate enough estimation of the oscillator strengths for the transition.

In Fig. 2 the "AA" bands after the γ-irradiation are shown for the samples S1,...S5. As seen from the figure these bands significantly differ. For samples S1, S3, S4 and S5, evident extrema (minima for S1 and S5 and maxima for S3 and S4) are observed on the broad background of the structureless band extending from the edge of the fundamental absorption up to λ=700 nm. Their shape and position coincide with the absorption bands caused by transitions between different configurations in Ce^{3+} ions. In the AA spectrum for sample S2, only a broad structureless band is observed, without any singularities.
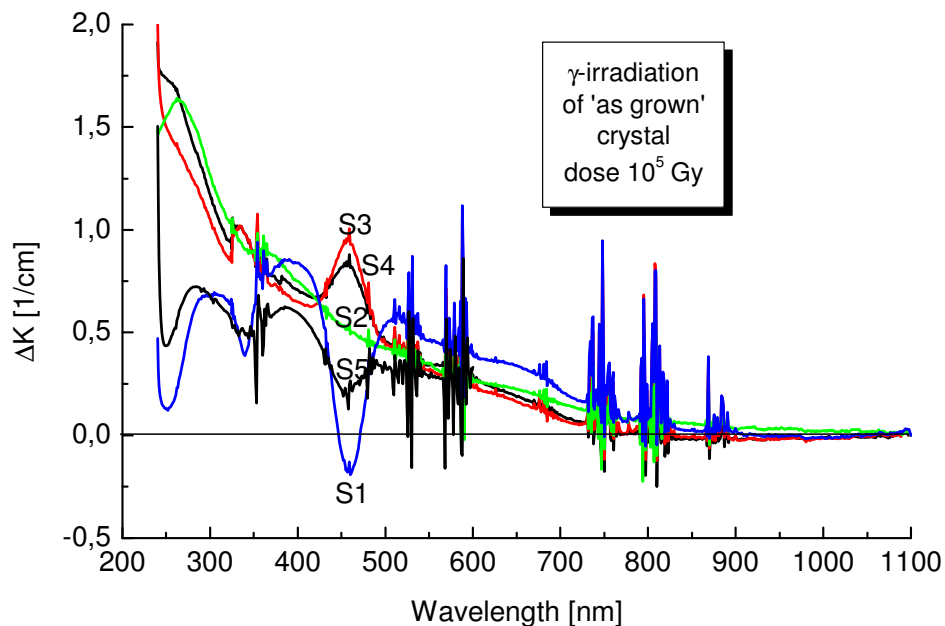
Fig. 2

In Fig. 3 the "AA" spectra obtained during thermal treatement of the samples S1,..S4 at $1400^{o}C$ in air are shown. The AA-bands for samples S1, S3 and S4 after thermal treatement have features opposite to those obtained after the gamma irradiation: in sample S1, a maximum of AA is observed in the absorption region of Ce^{3+}, while in samples S3 and S4 - the corresponding mimima are present. In sample S2, practically no changes are observed in the Ce^{3+} absorption range.

The AA-bands show that in samples S1, S3 and S4, under the influence of gamma radiation and under thermal processing, changes of Ce^{3+} concentrations take place. Results of calculations of the relative changes of Ce^{3+} concentrations after irradiation are shown in the table. In sample S2, no changes of the Ce^{3+} density are observed.

One can obtain the same results comparing AA bands after annealing the same sample
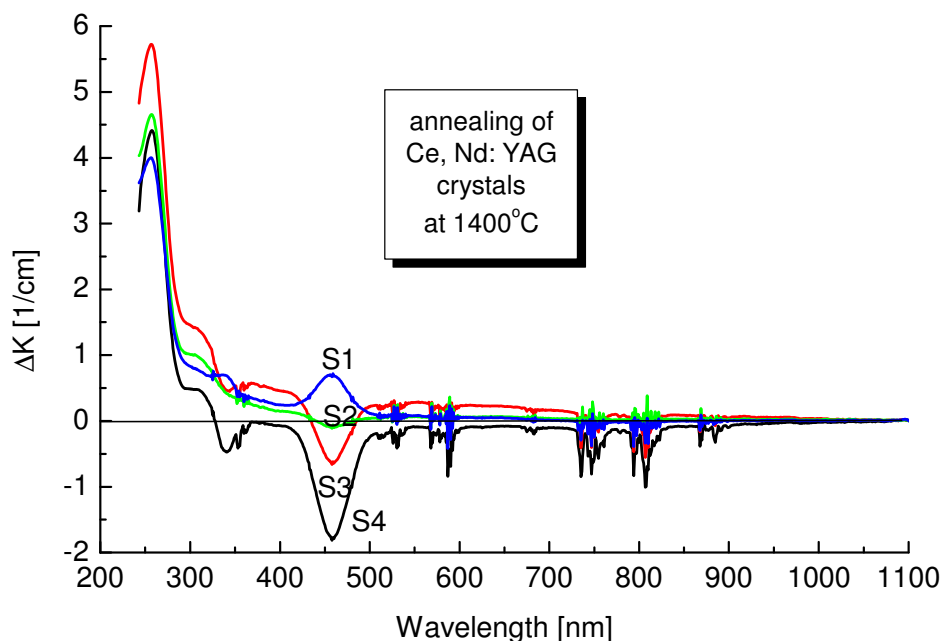
Fig. 3

(S4) in air and in an N_2+H_2 mixture, and comparing AA bands for γ-irradiation of the same sample (S4) as grown and after annealing in an N_2+H_2 mixture. Corresponding curves are presented in Fig. 4.

In Fig. 5 the AA spectra obtained after proton irradiation of sample S5 (irradiation after thermal annealing) are shown. As can be seen, another type of irradiation (immediate ionization) leads to AA bands, where, in the case of the first dose (10^{13} protons/cm^2), one can distinguish the $Ce^{3+} \rightarrow Ce^{4+}$ ionization process. In the second dose ($3*10^{13}$ protons/cm^2), the concentration of Ce^{3+} ions increases. Under the third dose (10^{14} protons/cm^2) the above mentioned process reverses.

In this figure one can also see electron-irradiation influence on the Ce:YAG crystal ($0,05$at.% Ce^{3+}) in the over-threshold type interaction (energy of particles ~1MeV). One can see that values of AA are much greater then after gamma and proton

irradiation and that for 458 nm AA decreases (the ionization process $Ce^{3+} \rightarrow Ce^{4+}$ takes place).

4. Discussion

The above results can be explained as follows. For given growth conditions (e.g. growth method, purity of the starting material, growth atmosphere, technological parameters) some definite sub-system of point defects appears in the crystal (e.g.doping ions, vacancies or interstitial defects). At the end of the growth process it is electrically balanced and is left in a metastable state. Some external factors, like irradiation or thermal processing, may lead to the transition of this subsystem from one metastable state to another. During this transition point defects may change their charge state.

Reasoning along this line one can guess that in samples S1 and S5, where Ce^{3+} concentration is small, the state of the subsystem is such, that after the excitation of the crystal by gamma radiation part of the Ce ions pass from the trivalence state to another one, most probably to Ce^{4+}. In sample S2 the ratio Ce^{3+}/Ce^{4+} doesn't change. In samples S3 and S4 radiative recharging of the Ce ions goes in the opposite direction $Ce^{4+} \rightarrow Ce^{3+}$.

In sample S5, under proton ionization, change of charge state $Ce^{3+} \rightarrow Ce^{4+}$ is more evident and dependent on the radiation dose.

Mutually reversible changes of the charge state, $Ce^{3+} \leftrightarrow Ce^{4+}$, were observed earlier in

Lu_2O_3: Ce crystals during heating in various atmospheres [11]. In this work it was also shown that the appearance of Ce^{4+} ions in the YAG crystal increases absorption in the

range of spectra with $\lambda < 350$ nm, where the charge transport band between oxygen

ions and Ce^{4+} exists. An analogous picture is observed also in our samples.

5. Conclusions

The presence of Ce^{4+} ions in the as grown Ce, Nd: YAG (also in Ce:YAG's)
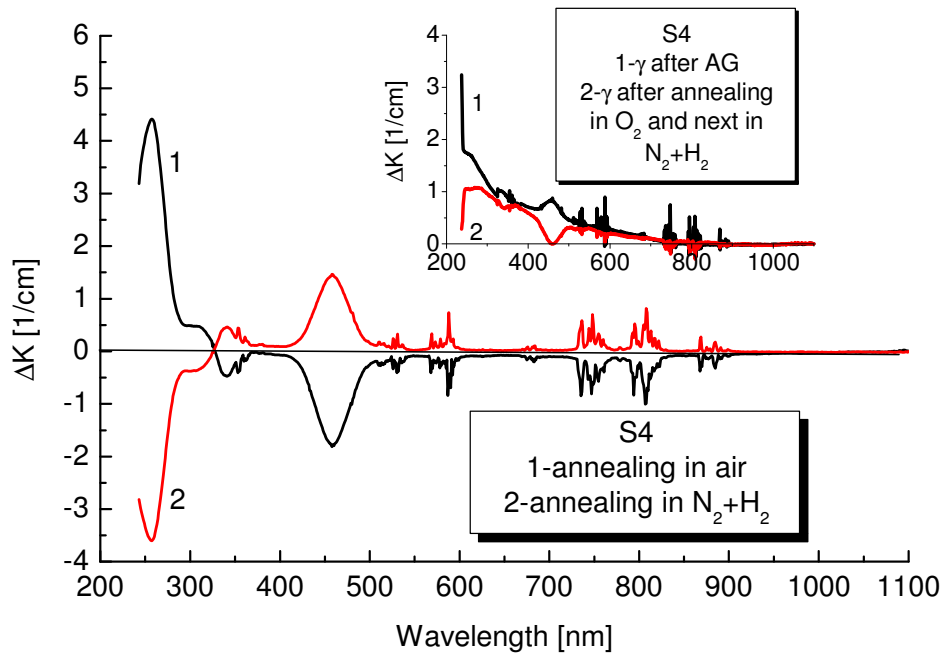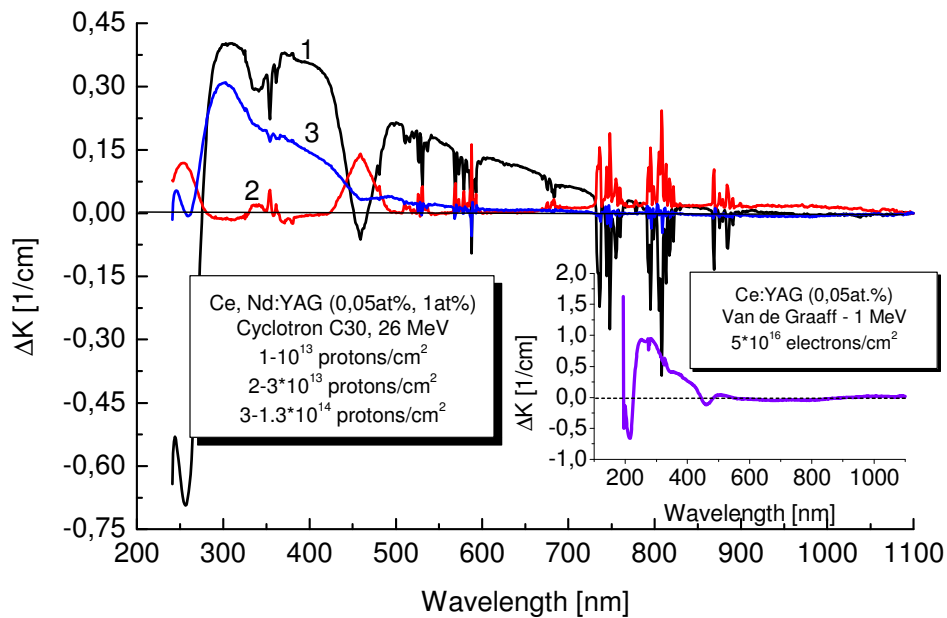
single

Fig. 4.

Fig. 5

crystals can be explained by the fact that if, during the synthesis, cerium dioxide (CeO_2) is used as the starting material, not all of the Ce ions pass to the tri-valent state.

The appearance of the broad background band observed in the AA-spectrum can be explained by the production of other colour centers (F-type centers, hole centers in the vincinity of the kation sub-lattice, recharging of the uncontrolled dopants etc.)

In conclusion, it was experimentally observed that under gamma and proton irradiation as well as in thermal processing, a change of the concentration of Ce^{3+} ions takes place in Ce, Nd: YAG crystals, as a result of recharging processes of the type $Ce^{4+} \leftrightarrow Ce^{3+}$.

6. Acknowledgements

References

1. A.O. Matkovskii, D.J. Sugak, S.B. Ubizskii, O.I. Shpotiuk, E.A. Chernyi, N.M. Vakiv and W.A. Mokryckii, in "Influence of an ionizing radiation on electron technics materials", in Russian, Svit, Lviv 1994, p. 212

2. M.R. Biedilov, H.B. Bejsembajeva, P.K. Habibulajev oraz R.P. Saidov, Ukr. Fiz. Zurn., in Russian, 31(1) (1986) 59

3. G.N. Pirogova, W.E. Krickaja, N.A. Anisimov oraz L.G. Demiashkina, Neorg. Mater., in Russian, 11(10) (1975) 1812

4. J. Kvapil, Jos. Kvapil, B. Perner, J. Kubelka, B. Manek oraz V. Kubecek, Czech. J. Phys. B, 34 (1984) 581

5. J. Mares, Czech. J. Phys. B, 35 (1985) 883

6. N. S. Kovaleva, A. O. Ivanov oraz E. P. Dubrovina, Kvantovaja Elektronika, in Russian, 8(11) (1981) 2433

7. T. Tomiki, H. Akamine, M. Gushiken, Y. Kinjoh, M. Miyazato, T. Miyazato, N. Toyokawa, M. Hiraoka, N. Hirata, Y. Ganaha oraz T. Futemma, J. Phys. Soc. Japan, 60(7) (1991) 2437

8. D. L. Dexter, Phys. Rev., 101(1) (1956) 48

9. A. A. Kaminskii, "Lasing crystals", Nauka, Moscow 1975, p. 215

10. G. A. Slack, S. L. Dole, V. Tsoukala oraz G. S. Nolas, J. Opt. Soc. Am. B, 11(6) (1994) 961

11. W. M. Yen, S. Basun, U. Happek oraz M. Raukas, Acta Physica Polonica A, 90(2)

    (1996) 257

Figure captions

Fig. 1. Absorption coefficient of Ce, Nd:YAG (0,05at.% Ce^{3+}, 1at.% Nd^{3+}) crystals

(samples S1,...S5) in the range of 200-1100nm.

Fig. 2 Additional absorption bands of Ce, Nd:YAG as grown crystals irradiated by

gamma rays with dose of 10^5 Gy.

Fig. 3 Additional absorption bands in 1400°C thermally annealed in air Ce, Nd: YAG

crystals.

Fig. 4. AA bands of Ce, Nd: YAG crystal (S4) for annealing in air compare to

annealing in an N_2+H_2 mixture. Small figure presents AA bands after γ-irradiation of

as grown Ce, Nd:YAG crystal (S4) compare to the same crystal annealed in an N_2+H_2

atmosphere.

Fig. 5 AA bands for Ce, Nd: YAG crystal after annealing in air and proton irradiation

with doses from $1*10^{13}$ to $1,3*10^{14}$ protons/cm^2. Small figure presents AA bands in

Ce:YAG (0,05at.%) crystal after electron irradiation with fluence $5*10^{16}$

electrons/cm^2.

Table: Parameters of the absorption band of the Ce^{3+} ions with maximum at 458 nm and calculated values of the Ce^{3+} concentrations before and after gamma irradiation for samples S1,...,S5 of Ce, Nd: YAG crystal.

Sample no.	K [cm^{-1}]	W [eV]	N_{Ce}[at.%} before	N_{Ce}[at.%} after irrad.	$\Delta N=[(N_{after}-N_{before})/N_{before}]*100\%$
S1	1,43	0,212	0,0040	0,0021	-48,1
S2	3,93	0,237	0,0122	0,0122	0
S3	4,40	0,234	0,0135	0,0149	10,1
S4	5,04	0,237	0,0157	0,0167	6,27
S5	2,53	0,219	0,0073	0,0062	-15,3